PHONONIC CRYSTALS

Direct observation of Klein tunneling in phononic crystals

Xue Jiang[1,2]*, Chengzhi Shi[1,3]*, Zhenglu Li[4,5], Siqi Wang[1], Yuan Wang[1], Sui Yang[1], Steven G. Louie[4,5], Xiang Zhang[1,6]†

Tunneling plays an essential role in many branches of physics and has found important applications. It is theoretically proposed that Klein tunneling occurs when, under normal incidence, quasiparticles exhibit unimpeded penetration through potential barriers independent of their height and width. We created a phononic heterojunction by sandwiching two types of artificial phononic crystals with different Dirac point energies. The direct observation of Klein tunneling as shown by the key feature of unity transmission is demonstrated. Our experiment reveals that Klein tunneling occurs over a broad band of acoustic frequency. The direct observation of Klein tunneling in phononic crystals could find applications in signal processing, supercollimated beams, and communications.

One of the most intriguing phenomena in quantum mechanics is the tunneling of a relativistic Dirac particle with a unity transmission that is independent of the width and height of a barrier upon normal incidence. This counterintuitive phenomenon is known as Klein tunneling, in marked contrast to the tunneling effect in nonrelativistic limit, where the normal transmission probability is hindered by the specifics of the barriers. Although theoretically proposed by Oskar Klein in 1929 for high-energy electrons (*1*), the experimental realization of Klein tunneling was an intractable challenge in particle physics because of the stringent requirements of accelerating a particle to a relativistic regime and constructing a parallel barrier (*2*).

Recently, a graphene monolayer was found to contain quasiparticles with massless relativistic dispersion known as the Dirac cone band structures (*3*–*8*). However, only some indirect features of Klein tunneling were deduced from the measurement of electrical resistance (*9*, *10*). Another signature was seen from the conductance oscillation and the half-period phase shift in a perpendicular magnetic field (*11*, *12*). However, the unambiguous evidence of Klein tunneling, i.e., unity normal transmission that is independent of the height and width of the energy barrier, has yet to be observed. The difficulties lie in the stringent and simultaneous requirements (*11*) of disorder-free heterojunction working in the ballistic regime, a highly collimated electron beam, and the potential barrier with parallel interfaces. Thus far, direct experimental demonstration of Klein tunneling has remained an outstanding quest.

We report here the observation of Klein tunneling by direct accessing of its key feature of unity normal transmission. Analogously to chemical or electrical gate doping in a graphene system, we used a phononic crystal (*13*–*22*) and achieved acoustic doping by synthesizing and sandwiching two types of artificial phononic crystals with different Dirac point energies. This naturally forms the required n-p-n–like heterostructure. The energy barrier height can be easily controlled by changing the unit cell geometry of the sandwiched phononic crystal. In addition, we demonstrate the effective broad frequency range of Klein tunneling. Such a direct experimental confirmation of Klein tunneling in a phononic system provides a promising platform with which to explore complex, nontrivial physics that usually require challenging delicate fabrications of samples in electronic systems.

Klein tunneling in condensed-matter systems is rooted in momentum-pseudospin locking and conservation of the pseudospin

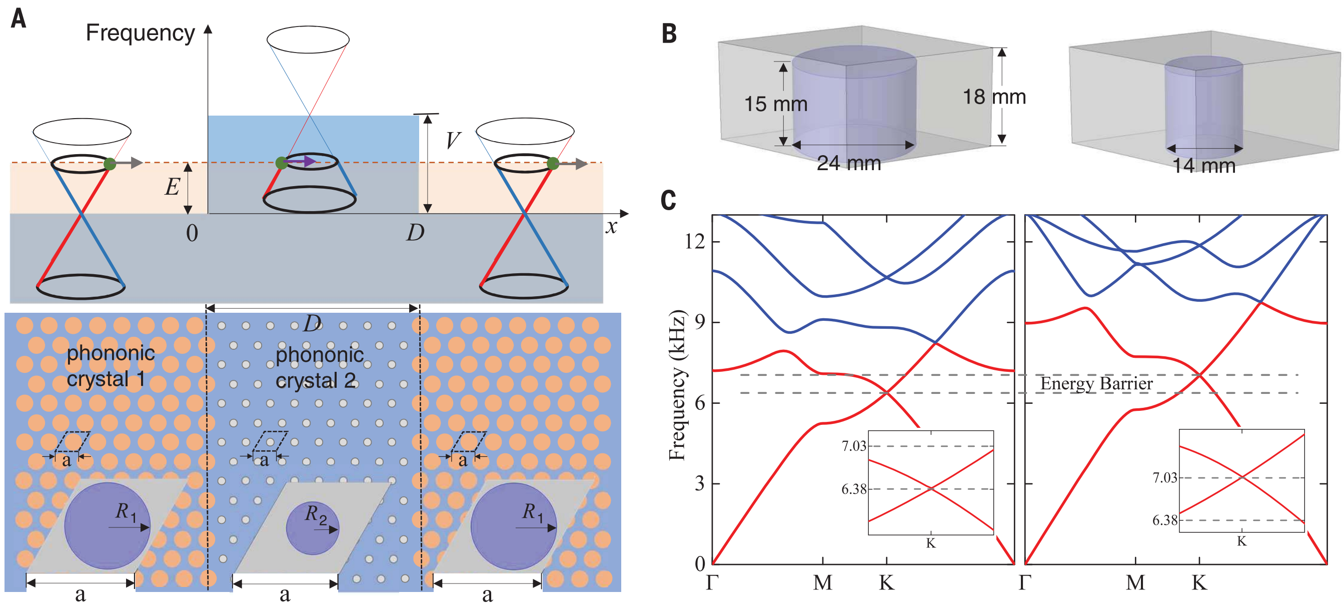

Fig. 1. Klein tunneling in barrier structure formed by Dirac phononic crystals. (**A**) Schematic of the conical spectrum of Klein tunneling (top panel), with a potential barrier of width *D* and height *V*. The red and blue lines denote the linear crossing branches with opposite pseudospin, resembling a massless relativistic Dirac quasiparticle. The green dots represent the Dirac quasiparticles with directions of motion that remain the same because of the conservation of pseudospin, indicated by gray and purple arrows. The bottom panel is the phononic heterostructure constructed by two triangular lattices. Schematics of the unit cells are shown in (**B**), with (**C**) showing the corresponding band structures forming a potential barrier height of 652 Hz (the energy separation between the two Dirac points located at 6380 and 7032 Hz, respectively). The gray dashed lines indicate the position of the Dirac points, and the insets show the zoom-in plots.

in the scattering of massless Dirac quasiparticles. This pseudospin physics fundamentally represents the relative phase of the excitation amplitude on two real-space sublattices of the eigenmodes of the Dirac quasiparticles (*5*) in the long-wavelength limit (i.e., the length scale is large compared with the interatomic distance). A typical one-dimensional potential barrier with height V and width D can be synthesized by lifting the Dirac point excitation energy in the sandwiched spatial region above that in the outer regions forming the Dirac heterojunction (Fig. 1A). In the classical picture, a particle traveling with energy lower than the barrier height will be completely back scattered; for a nonrelativistic particle in the same scenario, the normal transmission amplitude will decay exponentially with the width and height of the potential barrier. However, normal incident massless Dirac particles encountering the barrier will experience perfect transmission (Klein tunneling) made possible by the conservation of pseudospin of the Dirac quasiparticles. The backscattered particle has opposite pseudospin, and a potential in the long-wavelength limit cannot flip it (*4*, *23*).

The massless Dirac quasiparticles in our case are acoustic excitations from triangular phononic lattice with rigid cylinders, where the linear dispersed Dirac cones are formed near the K and K′ points at the Brillouin corners. We sandwiched two artificial phononic crystals with the same lattice constant but different cylinder radii (R). The Dirac point energies were purposely controlled by changing R (*24*), which serves as an important tuning parameter similar to (but more controllable than) the gating effect used in graphene systems. In our experiments, the geometric parameters were as follows: a = 28 mm, R_1 = 12 mm, and R_2 = 7 mm, where a, R_1, and R_2 are the common lattice constant and the cylinder radii of the two different crystals, respectively. The unit cell has a height of 15 mm, with an air gap of 3 mm left between the cylinder top and the upper cover for the field scanning (Fig. 1B). The calculated band structures of the two phononic crystals manifest linear dispersions, as illustrated in Fig. 1C, where a potential barrier of height V = 652 Hz is formed (*24*).

Klein tunneling manifests as the combination of three fundamental conservation laws. First, the conservation of energy E is a result of time-translational invariance in a linear system, which requires the frequencies of the transmitted and incident waves to remain constant. Second, because of spatial translation symmetry along the interface, the normal-incident quasiparticles conserve their transverse momentum along y (parallel to the interfaces), namely $k_y = 0$. The third relevant conservation law here is pseudospin conservation, which forbids the back scattering for incidence at the normal direction. Therefore, the incident acoustic wave should be transmitted through the potential barrier with unity transmission regardless of the width and height of the barrier (*11*).

An acoustic plane wave at 6800 Hz was excited across the Dirac heterostructure at normal incidence. At this excitation frequency, phononic crystals 1 (2) correspond to the n-doped (p-doped) regime (Fig. 2A). The transmission dependence of the barrier width D was measured (Fig. 2B), with fixed barrier height V = 652 Hz. The measured region is indicated by

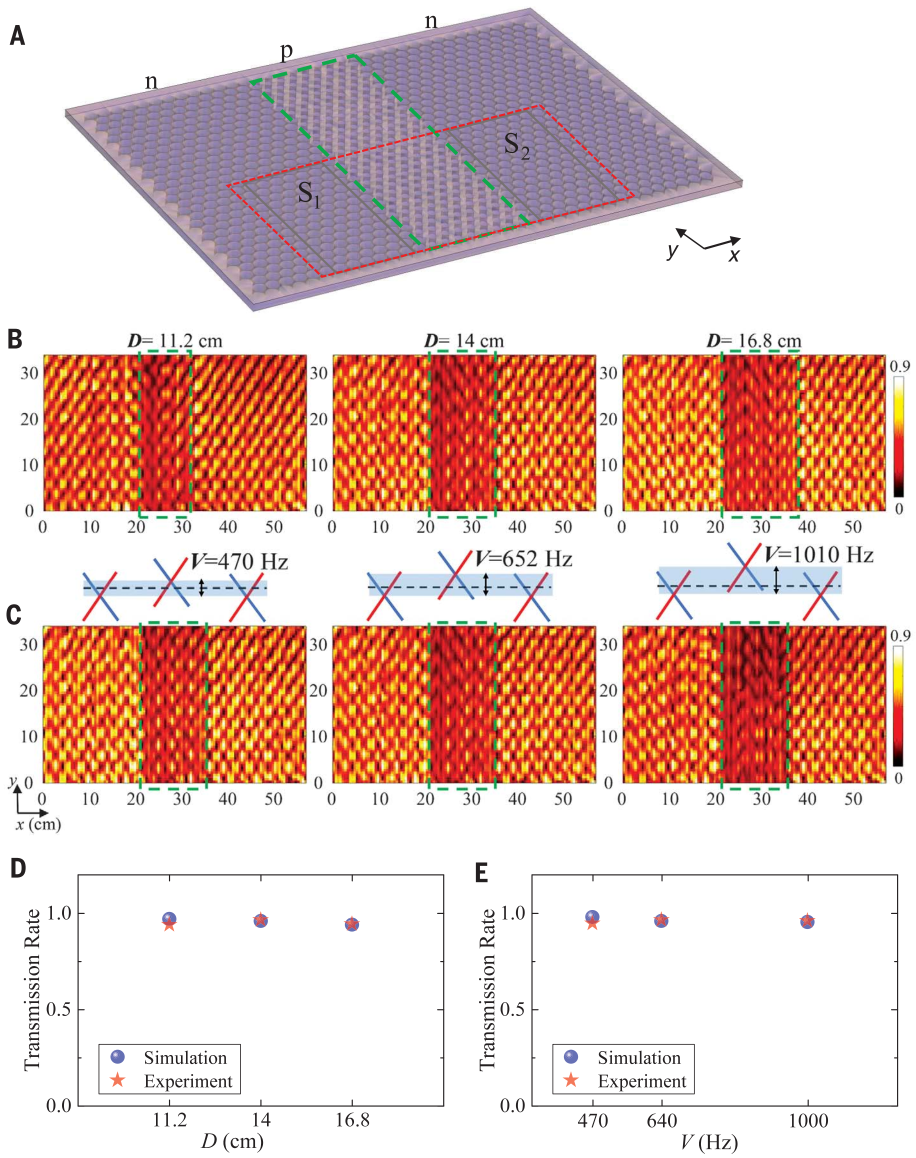

Fig. 2. Normal transmission measured independent of potential width and height. (**A**) Schematic of Klein tunneling measurement. Field scanning was performed over the n-p-n heterojunction. The green, red, and gray boxes indicate the potential barrier, the measured region, and the areas for calculation (*24*), respectively. (**B**) Experimentally measured amplitude of the normalized pressure field at normal incidence. Frequency f = 6800 Hz and potential barrier V = 652 Hz were fixed while varying barrier width D. (**C**) Amplitude of the normalized pressure field with fixed barrier width D = 14 mm and different potential height V. (**D** and **E**) Measured transmission rate of pressure amplitude as a function of the barrier width D and height V compared with the simulation results; estimated errors are smaller than the size of the markers.

[1]Nano-scale Science and Engineering Center, University of California, Berkeley, CA 94720, USA. [2]Department of Electronic Engineering, Fudan University, Shanghai 200433, China. [3]School of Mechanical Engineering, Georgia Institute of Technology, Atlanta, GA 30332, USA. [4]Department of Physics, University of California, Berkeley, CA 94720, USA. [5]Materials Sciences Division, Lawrence Berkeley National Laboratory, Berkeley, CA 94720, USA. [6]Faculty of Science and Faculty of Engineering, The University of Hong Kong, Hong Kong, China.
*These authors contributed equally to this work.
†Corresponding author. Email: president@hku.hk

the red dashed box in Fig. 2A, and the position of the potential barrier is indicated by the green dashed boxes. The pressure amplitude was normalized to the field without junction, namely, the triangular lattice consisting of the same cylinders, to eliminate unavoidable effect of sound diffusion (*24*). In Fig. 2B, it can be seen that the incident acoustic wave transmits through the barrier without changing patterns. To extract the transmission rate of the pressure amplitude, the integral (of the pressure amplitude) over the regions S_1 and S_2 (of the same area) before and after the potential barrier was performed (*24*).

Figure 2D shows the experimentally measured transmission rate as a function of barrier width *D*. The transmission was measured to be 94.3, 96.7, and 94.6% for *D* = 11.2 mm, 14 mm, and 16.8 cm, respectively, which is consistent with the 97.1, 96.0, and 93.8% found in theoretical simulations using the finite element method (*24*). The pressure amplitudes inside and outside the barrier are different because of the different effective acoustic impedance (Z_{eff}) in the two phononic crystals. However, the two n-doped regimes before and after the barrier contain the same Z_{eff}, and thus the perfect transmission of acoustic pressure *p* is equivalent to the near-unity transmission of acoustic intensity: $I = |p|^2/Z_{eff}$, which represents the energy flux.

Furthermore, the potential height *V* can be easily tuned by changing the cylinder radius R_2 in the barrier. Here, three cylinders with the radii of R_2 = 5, 7, and 8.25 mm lead to barriers of heights *V* = 470, 652, and 1010 Hz, respectively, and the barrier width is fixed to be *D* = 14 mm. The measured pressure amplitude fields are given in Fig. 2C, and the transmission rate is shown in Fig. 2E as a function of *V*. The transmission rate is 95.2, 96.7, and 96.2% for *V* = 470, 652, and 1010 Hz in the experiment and 98.9, 96.0, and 95.8% in the simulations, respectively. Direct evidence of Klein tunneling is unity normal transmission, which has long been pursued in experimental observations. The previous measurements on electronic resistance or phase shift (*9*, *10*, *12*) have not shown direct evidence of unity transmission, although they may indicate some features of Klein tunneling (*11*). In our work, near-unity transmission was observed regardless of the width and height of the potential barrier, which gives a direct experimental demonstration of Klein tunneling. The transmission measured experimentally being not exactly at unity described by theory may result from experimental conditions that were not absolutely ideal, from small sample fabrication imperfections, to finite-size unit cell effect, to the theoretically required infinite-size crystals on both sides of the junction. Nevertheless, the physics of Klein tunneling were clearly demonstrated in this experiment.

The advantage of studying artificial phononic crystals is that the type of tunneling probed can be freely tailored by the excitation frequencies. This is because a given potential barrier can correspond to different types of Dirac/non-Dirac heterojunctions depending on the excitation frequency used: There will be a bipolar n-p-n junction if the excitation frequency lies in different (upper versus lower) Dirac cones inside and outside the barrier (yellow zone in Fig. 3A), but a unipolar p-p′-p or n-n′-n junction if it lies in the same Dirac cone (magenta zone in Fig. 3A). Both the bipolar and unipolar junctions are of the proper geometries to support Klein tunneling. It should also be noted that the quasi-particle gradually acquires nonlinearity in the dispersion relation when the excitation frequency is tuned away from the energy of the Dirac point (gray and purple zones in Fig. 3A).

Experimentally, we tuned the excitation frequency into these four dispersion regions (indicated by the colored dots in Fig. 3A). The measured pressure fields across the same potential barrier (*D* = 14 mm and *V* = 652 Hz) with different excitation frequencies are shown in Fig. 3C. A near-unity transmission plateau is observed over a broad frequency range (from 5800 to 6800 Hz). By contrast, the transmission drops substantially to 83.6 and 11.1% for *f* = 5200 and 7900 Hz, respectively, where these particles no longer support Klein tunneling because the pseudospin-momentum locking

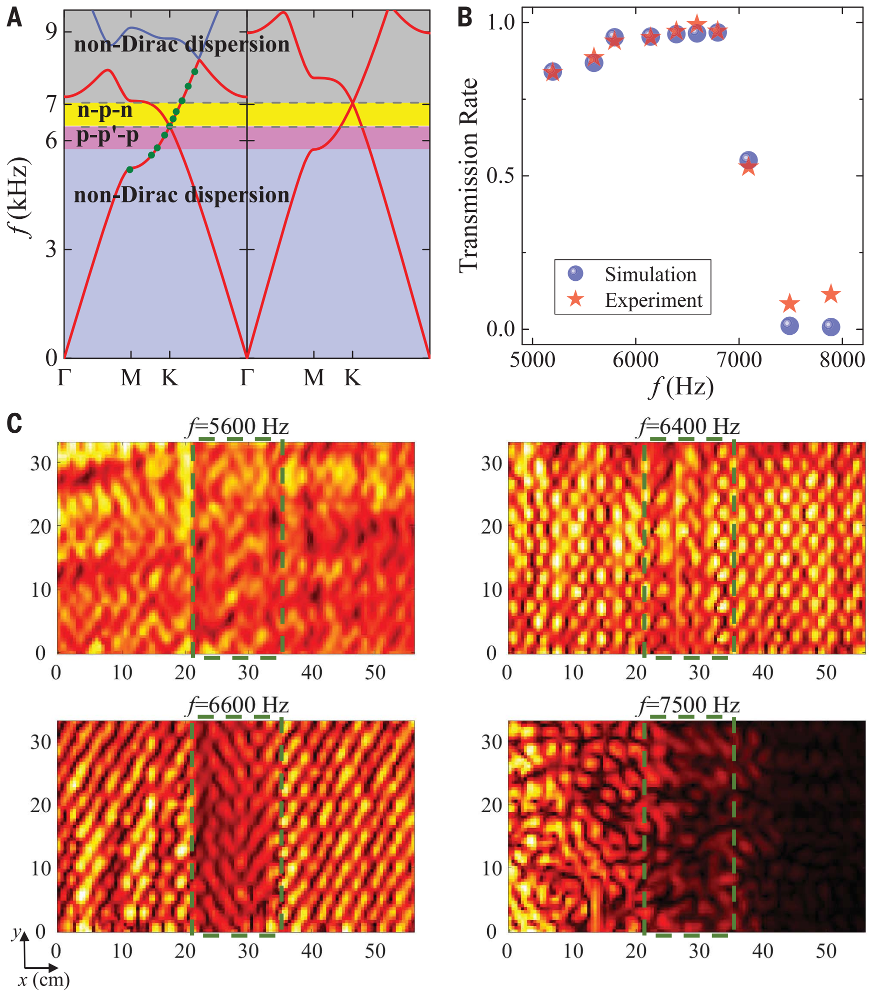

Fig. 3. Observation of Klein tunneling over a broad frequency band. (**A**) Left and right panels show the dispersion relation of two phononic crystals with different radii (refer to Fig. 1C). Depending on the excitation frequency, the potential barrier corresponds to different types of junctions. The dots indicate the frequencies picked in the following comparison. (**B**) Frequency-dependent transmission rate. Within the linear dispersed range of both crystals, the transmission at normal incidence approaches unity. The estimated errors are smaller than the size of the markers. By contrast, the transmission drops rapidly in the nonlinear dispersion range. (**C**) Experimentally measured amplitude of the normalized pressure fields at different frequencies.

feature does not associate with states far away from the Dirac point.

We have demonstrated direct observation of Klein tunneling, as evidenced by perfect transmission across a phononic crystal heterojunction structure upon normal incidence. Moreover, the frequency range for Klein tunneling can be explored by changing the excitation frequency of the incident acoustic wave and is controlled by the linear dispersed range of the two crystals away from their Dirac point energy. Our work presents a new platform for exploring emerging macroscale systems to be used in applications such as on-chip logic devices for sound manipulation, acoustic signal processing, and sound energy harvesting.

REFERENCES AND NOTES

1. O. Klein, *Z. Phys.* **53**, 157–165 (1929).
2. A. Calogeracos, N. Dombey, *Contemp. Phys.* **40**, 313–321 (1999).
3. K. S. Novoselov *et al.*, *Science* **306**, 666–669 (2004).
4. M. I. Katsnelson, K. S. Novoselov, A. K. Geim, *Nat. Phys.* **2**, 620–625 (2006).
5. C.-H. Park, S. G. Louie, *Nano Lett.* **9**, 1793–1797 (2009).
6. X. Huang, Y. Lai, Z. H. Hang, H. Zheng, C. T. Chan, *Nat. Mater.* **10**, 582–586 (2011).
7. J. Mei, Y. Wu, C. T. Chan, Z.-Q. Zhang, *Phys. Rev. B Condens. Matter Mater. Phys.* **86**, 035141 (2012).
8. C.-H. Park, L. Yang, Y. W. Son, M. L. Cohen, S. G. Louie, *Nat. Phys.* **4**, 213–217 (2008).
9. B. Huard *et al.*, *Phys. Rev. Lett.* **98**, 236803 (2007).
10. R. V. Gorbachev, A. S. Mayorov, A. K. Savchenko, D. W. Horsell, F. Guinea, *Nano Lett.* **8**, 1995–1999 (2008).
11. P. E. Allain, J. N. Fuchs, *Eur. Phys. J. B* **83**, 301–317 (2011).
12. A. F. Young, P. Kim, *Nat. Phys.* **5**, 222–226 (2009).
13. Z. Yang *et al.*, *Phys. Rev. Lett.* **114**, 114301 (2015).
14. A. B. Khanikaev, R. Fleury, S. H. Mousavi, A. Alù, *Nat. Commun.* **6**, 8260 (2015).
15. C. He *et al.*, *Nat. Phys.* **12**, 1124–1129 (2016).
16. Y. Liu, C.-S. Lian, Y. Li, Y. Xu, W. Duan, *Phys. Rev. Lett.* **119**, 255901 (2017).
17. J. Lu, C. Qiu, M. Ke, Z. Liu, *Phys. Rev. Lett.* **116**, 093901 (2016).
18. Z. Zhang *et al.*, *Phys. Rev. Lett.* **118**, 084303 (2017).
19. M. Xiao, W.-J. Chen, W.-Y. He, C. T. Chan, *Nat. Phys.* **11**, 920–924 (2015).
20. F. Li, X. Huang, J. Lu, J. Ma, Z. Liu, *Nat. Phys.* **14**, 30–34 (2018).
21. X. J. Zhang, M. Xiao, Y. Cheng, M. H. Lu, J. Christensen, *Commun. Phys.* **1**, 97 (2018).
22. M. Dubois, C. Shi, X. Zhu, Y. Wang, X. Zhang, *Nat. Commun.* **8**, 14871 (2017).
23. A. H. Castro Neto, F. Guinea, N. M. R. Peres, K. S. Novoselov, A. K. Geim, *Rev. Mod. Phys.* **81**, 109–162 (2009).
24. See the materials and methods in the supplementary materials.

ACKNOWLEDGMENTS

Funding: This work was supported by the Gordon and Betty Moore Foundation (award no. 5722), the King Abdullah University of Science and Technology (KAUST Office of Sponsored Research award no. OSR-2016-CRG5-2996), the National Natural Science Foundation of China (grant no. 11904055), and the Young Elite Scientists Sponsorship Program by CAST. Z.L. and S.G.L. acknowledge support from the National Science Foundation (grant no. DMR-1926004). **Author contributions:** X.J. and C.S. performed experiments and numerical simulations. X.J. and Z.L. performed theoretical analyses. X.J., Z.L., S.Y., and X.Z. wrote the initial draft of the manuscript with the input of S.W. and Y.W. S.G.L. supervised the theoretical analysis and X.Z. supervised the project. All authors analyzed the results and contributed to the manuscript. **Competing interests:** The authors declare no competing interests. **Data and materials availability:** All data are available in the main text or the supplementary materials.

SUPPLEMENTARY MATERIALS

science.sciencemag.org/content/370/6523/1447/suppl/DC1
Materials and Methods
Supplementary Text
Figs. S1 to S8
References

6 August 2020; accepted 18 November 2020
10.1126/science.abe2011

Science

Direct observation of Klein tunneling in phononic crystals

Xue Jiang, Chengzhi Shi, Zhenglu Li, Siqi Wang, Yuan Wang, Sui Yang, Steven G. Louie and Xiang Zhang

Science **370** (6523), 1447-1450.
DOI: 10.1126/science.abe2011

A sound demonstration of Klein tunneling

The ability of particles to tunnel through barriers is an important property of quantum mechanical systems, and the extent of the effect is strongly dependent on the properties of the barrier. By contrast, Klein tunneling can exhibit unity transmission that is independent of the width and height of the energy barrier, but direct evidence for this effect remains elusive. Using a phononic system comprising a periodic array of dielectric pillars, Jiang *et al.* provide evidence for the direct observation of Klein tunneling. Near-unity transmission of acoustic excitations was observed across the barrier independently of its width and height. This ability to tune the effect by controlling the size of the junctions and the frequency of incident waves provides a promising platform to explore complex nontrivial physics and applications in signal processing and information communications.

Science, this issue p. 1447

Science (print ISSN 0036-8075; online ISSN 1095-9203) is published by the American Association for the Advancement of Science, 1200 New York Avenue NW, Washington, DC 20005. The title *Science* is a registered trademark of AAAS.